Spectral Light Quality and D-Limonene Modulate Plant Growth and Pharmacological Compounds in Mikania laevigata Sch.Bip. ex Baker

Maria Eduarda Almeida Souza , Victor de Oliveira Dias , Paulo Hercílio Viegas Rodrigues * , Júlio César Altizani-Júnior * , Guilherme Bovi Ambrosano , Luana Gonçalves Zamarrenho , Jéssica Aparecida de Lima , Andresa Aparecida Berretta

Posted Date: 17 June 2025

doi: 10.20944/preprints202506.1461.v1

Keywords: shade nets; foliar application; secondary metabolism; coumarin biosynthesis; spectral light manipulation; elicitation; photosynthetic activity; medicinal plants

 doi:10.20944/preprints202506.1461.v1

Article

Spectral Light Quality and D-Limonene Modulate Plant Growth and Pharmacological Compounds in *Mikania laevigata* Sch.Bip. ex Baker

Maria Eduarda Almeida Souza [1,†], Victor de Oliveira Dias [1,†], Paulo Hercílio Viegas Rodrigues [1,*], Júlio César Altizani-Júnior [1,*], Guilherme Bovi Ambrosano [2], Luana Gonçalves Zamarrenho [3], Jéssica Aparecida de Lima [3,4] and Andresa Aparecida Berretta [3]

[1] Department of Crop Science, "Luiz de Queiroz" College of Agriculture (ESALQ), University of São Paulo (USP), Piracicaba-SP, 13418-900, Brazil; maria.eduardaasz@usp.br (M.E.A.S.); victordeoliveiradias@usp.br (V.O.D); phrviegas@usp.br (P.H.V.R.); altizani@usp.br (J.C.A-J.)

[2] Department of Genetics, "Luiz de Queiroz" College of Agriculture (ESALQ), University of São Paulo (USP), Piracicaba-SP, 13418-900, Brazil; guilherme.ambrosano@usp.br (G.B.A)

[3] Laboratory of Research, Development and Innovation, Apis Flora Industrial and Commercial Limited, Ribeirão Preto-SP, 14020-670, Brazil; luana.zamarrenho@apisflora.com.br (L.G.Z); jesica.lima@apisflora.com.br (J.A.L); andresa.berretta@apisflora.com.br (A.A.B.)

[4] Pharmaceutical Sciences Department, Faculty of Pharmaceutical Sciences of Ribeirão Preto, University of São Paulo (FCFRP/USP), Ribeirão Preto-SP, Brazil; jesica.lima@apisflora.com.br (J.A.L)

* Correspondence: altizani@usp.br and phrviegas@usp.br

† These authors contributed equally to this work.

Abstract: The efficacy and safety of phytotherapeutic medicines are intrinsically related to the quality of their plant-based raw materials, which is directly influenced by agronomic cultivation practices. In this scenario, this study aimed to evaluate the effects of colored shade nets and foliar application of D-limonene on the growth and secondary metabolism of *Mikania laevigata* Sch.Bip. ex Baker. The experiment followed a completely randomized 4 × 5 split-plot design, with three photoselective shade nets (red, blue and black) compared to full sunlight (control) and five D-limonene doses (0.00, 0.25, 0.50, 1.00, and 2.00 mL L^{-1}). Our findings revealed significant effects on plant height, number of leaves, stem diameter, and leaf dry matter. The red net promoted greater shoot biomass accumulation and increased leaf dry mass. Regarding secondary metabolites, the red and black nets enhanced coumarin content by 18.80% and 15.36%, respectively, compared to full sunlight cultivation. D-limonene positively influenced biometric traits up to 1.20 mL·L^{-1}, followed by a decline. These findings indicate that colored shade nets could be an effective approach to enhance the phytochemical yield of *M. laevigata*, while D-limonene contributes mainly to morphological development and biomass accumulation.

Keywords: shade nets; foliar application; secondary metabolism; coumarin biosynthesis; spectral light manipulation; elicitation; photosynthetic activity; medicinal plants

1. Introduction

The escalating global demand for plant-derived therapeutic resources reflects rising confidence in traditional medicine, which critically contributes to primary healthcare and inspires the development of novel pharmaceuticals [1]. Indeed, over half of recently approved drugs originate from medicinal plants or their derivatives, underscoring their strategic relevance to public health initiatives [2]. Projections from the World Health Organization (WHO) estimate the global market for herbal medicines and plant-based products will reach USD 5 trillion by 2050 [1]. In this context, the adoption of agronomic strategies that ensure the efficient, standardized, and sustainable cultivation of these species represents a critical pathway to narrowing the gap between escalating demand and the limited supply of high-quality raw materials.

Brazil, with its remarkable biodiversity, holds substantial potential for developing value chains centered on native species possessing bioactive properties. However, this sector faces significant constraints, including prevalent extractive practices, limited adoption of Good Agricultural Practices

 doi:10.20944/preprints202506.1461.v1

(GAP), inadequate production standardization, and insufficient technical and policy support [3]. Furthermore, the underdeveloped organization of these chains, associated with minimal value addition at the production level, severely diminishes the economic and social benefits derived from these species [4]. Overcoming these challenges requires targeted research focused on strengthening the structure and integration of the medicinal plant sector in the country.

Among Brazil's native medicinal flora, *Mikania laevigata* Sch.Bip ex Baker., commonly known as *Guaco*, stands out for its pharmacological potential. This climbing herbaceous plant, a member of the Asteraceae family, naturally occurs in moderate-shaded environments of tropical rainforests [5]. Its therapeutic relevance has been acknowledged since the first edition of the Brazilian Pharmacopoeia [6], primarily due to its well-documented bronchodilator, anti-inflammatory, and expectorant properties [7,8]. These properties are predominantly attributed to the presence of key secondary metabolites, particularly coumarins [9–11]. Beyond its established phytotherapeutically importance, the species of this botanical genus also harbors beneficial microorganisms that can promote plant development and enhance cash crop performance [12].

Predominantly concentrated in the leaves, the coumarins are secondary metabolites synthesized through the shikimate pathway. This biosynthetic route initiates with the condensation of phosphoenolpyruvate and erythrose-4-phosphate [13], leading to the production of chorismic acid and subsequent synthesis of aromatic amino acids. Phenylalanine is converted by phenylalanine ammonia-lyase (PAL) into cinnamic acid, which is further transformed into o-coumaric acid. Through glycosylation, cis/trans isomerization, and lactonization, these intermediates give rise to coumarins [14]. Like other pharmacological molecules, the production of this compound is modulated by genetic background, environmental variables, and cultivation practices [15,16]. In this regard, Souza et al. (2010) [17] demonstrated that *M. laevigata* exhibits high metabolic plasticity, with secondary metabolite synthesis significantly influenced by environmental conditions.

Within these factors, light plays a central role in modulating photosynthesis, stress responses, and the expression of genes associated with specialized metabolism [18]. Contin et al. (2021) [19], for example, reported that light intensity directly affects the morphophysiological performance of *M. laevigata*, with enhanced photosynthetic efficiency, biometric parameters, and biomass accumulation observed under moderate shading. These findings emphasize the importance of managing light availability and understanding the environmental conditions of origin to optimize both plant development and secondary metabolite production in medicinal plants.

Moreover, a promising strategy to light manipulation involves the use of photoselective shade nets, such as ChromatiNET®®, which selectively filter the solar radiation and consequently influence plant morphogenesis, resource allocation, and metabolic activity [20,21]. For instance, according to the findings of Souza et al. (2011) [22], *Mikania glomerata* Sprengel plants cultivated under blue nets exhibited superior leaf expansion, dry matter production, and essential oil content compared to those under full sunlight, illustrating the potential of spectral manipulation to enhance the phytochemical yield.

In parallel, recent studies have investigated the elicitor potential of bioactive monoterpenes such as D-limonene ($C_{10}H_{16}$), a compound naturally found in essential oils. These molecules, categorized as elicitors of biotic or abiotic origin, stimulate plant defense responses and often induce the biosynthesis of specialized metabolites [23]. D-limonene has been shown to modulate physiological and metabolic processes related to plant development and secondary compound production [24,25]. In this sense, Orsi et al. [26] demonstrated that D-limonene application increased carotenoid accumulation during tomato ripening, suggesting its capacity to enhance specific metabolic pathways.

Thus, given the increasing demand from the pharmaceutical industry for raw materials with standardized coumarin content, this study aimed to evaluate the combined effects of D-limonene foliar application and colored shade nets on the growth and specialized metabolism of *M. laevigata*. Specifically, our objectives were to investigate: (i) biometric parameters and biomass production; (ii) the synthesis of photosynthetic pigments; and (iii) the accumulation of pharmacologically relevant secondary metabolites, including coumarins, flavonoids, and anthocyanins.

2. Materials and Methods

2.1. Experimental Conditions, Greenhouse Setup and Climatic Data

 doi:10.20944/preprints202506.1461.v1

The experiment was carried out under four light environments (three within a greenhouse and one in open-field conditions) at the experimental area of the Department of Crop Science at the "Luiz de Queiroz" College of Agriculture, University of São Paulo (ESALQ/USP), located in Piracicaba-SP, Brazil (Lat. 47°37′44 W, Long. 22°42′31 S, 546 m altitude) (Figure 1A,B). According to the Köppen climate classification, the region presents a Cwa climate: a subtropical type characterized by hot, wet summers and dry winters [27].

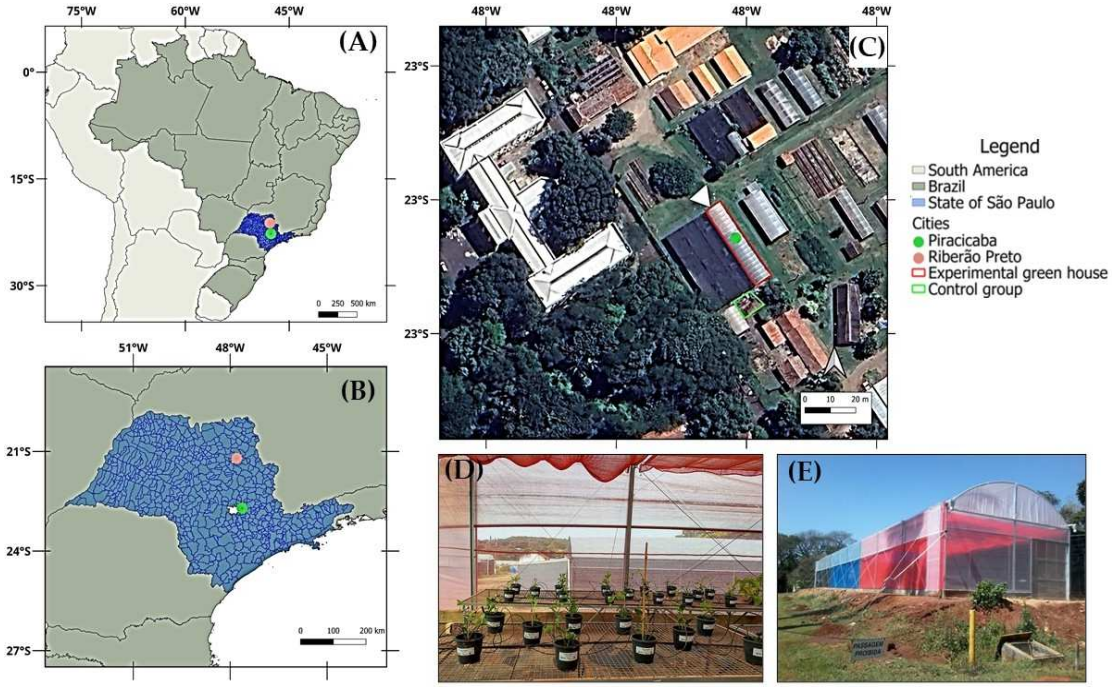

Figure 1. Locations of the experimental greenhouse in Piracicaba-SP and the laboratory in Ribeirão Preto-SP where coumarin analyses were conducted (A, B); aerial-satellite view of the experimental greenhouse and location of the control treatment (C); internal view of the reticulated-shade net (10 days after transplanting) as an example for showing the arrangement of experimental units (D); and external ground-level view of the greenhouse to demonstrate the disposition of the colored shade nets (E).

The experimental units were installed in a single-span greenhouse (6.4 m wide × 36 m long) covered with a light-diffusing polyethylene film (nominal 100% light transmissivity). Three light environments were created using photoselective shade nets (ChromatiNET®®, Ginegar; 5 mm thickness, nominal 50% shading): red, blue, and black. The north-south oriented greenhouse was internally divided into three equal sections, each covered with one colored net. To prevent light interference during the early hours of the day, the west side of each section was also covered with a net of the same color as the respective treatment. Additionally, a fourth light condition was implemented in an adjacent open-field area under full sunlight, serving as the control (Figure 1C,E).

Seedlings of *M. laevigata* were obtained from Flora Arco-Íris (Atibaia-SP, Brazil), a nursery specialized in ornamental and medicinal plants. The commercial origin of the material provides a reasonable assurance of species identity, minimizing the risk of confusion with other congeneric medicinal species. Uniformity in size and leaf number was used as a selection criterion to ensure initial homogeneity. On October 2, 2024, the seedlings were transplanted into 1.8 L pots filled with a commercial substrate (Basaplant Hortaliças®®, Base Substratos), composed of pine bark, peat, charcoal, and vermiculite. Basal fertilization consisted of 15 g per pot of controlled-release fertilizer (Basacote®® Plus 6M, COMPO EXPERT; 16-8-12 NPK). A drip irrigation system was used for all treatments, including the control group cultivated outdoors. The system consisted of PVC main lines and polyethylene lateral lines equipped with 2.0 $L \cdot h^{-1}$ pressure-compensating drippers connected to microtubes and two drip sticks at each pot outlet. Plants received two daily irrigations of 2 minutes each, at 06:00 and 18:00 h. Additionally, 15 days after transplanting (DAT), plants were staked using bamboo rods and tied with twine to ensure upright growth and prevent mechanical damage (Figure 1D).

 doi:10.20944/preprints202506.1461.v1

Daily meteorological conditions during the experimental period (October 2 to November 29, 2024) are presented in Table 1. For external monitoring, data was obtained from the ESALQ/USP weather station, located approximately 300 m from the experimental site. Inside the greenhouse, microclimatic monitoring was performed independently in each light environment using three automated weather stations. Each station was equipped with a CR1000 data logger (Campbell Scientific®®), an HMP45C sensor (Vaisala®®) for temperature and relative humidity, a CS100 barometric pressure sensor, and an LI200X silicon photodiode pyranometer (LI-COR®®) to measure global solar radiation. It is important to highlight that Pyranometer data were recorded in millivolts and converted to $MJ \cdot m^{-2} \cdot day^{-1}$ using a calibration factor of 0.0075 $V \cdot (MJ \cdot m^{-2} \cdot day^{-1})^{-1}$, following the validated methodology proposed by Freire et al. (2024) [21]. This method, based on the comparison with a reference Eppley pyranometer under clear-sky conditions, demonstrated strong linearity and accuracy, with coefficients of determination ranging from 0.98 to 0.99, confirming its suitability for precise solar radiation measurements.

Table 1. Average values of maximum and minimum air temperature, relative humidity, global solar radiation, and accumulated rainfall under different light environments (external conditions and colored shade nets) recorded from October 2 to November 29, 2024.

Treatments	Temperature (°C)		Relative humidity (%)		Global radiation (MJ m^{-2} day^{-1})		Rainfall (mm)
	Min	Max	Min	Max	Min	Max	Total
External	18.04	26.19	25.37	97.53	6.90	16.51	195
Red net	20.04	28.02	21.34	96.21	4.95	10.37	0
Black net	20.09	28.54	19.93	96.08	3.80	9.10	0
Blue net	19.24	27.44	21.72	96.04	2.40	5.78	0

2.2. Experimental Design and Applied Treatments

The study was conducted using a completely randomized design arranged in a 4 x 5 split-plot scheme. The main plots corresponded to four light conditions: red, blue, and black ChromatiNET®® shade nets, and full sunlight (open-field control). The subplots consisted of five D-limonene concentrations: 0.00, 0.25, 0.50, 1.00, and 2.00 $mL \cdot L^{-1}$. Each light environment contained 25 plants, with five plants allocated to each D-limonene dose. Each plant represented a single experimental unit, totaling 100 plants across all treatments. Pots were arranged on aluminum benches with approximately 40 cm spacing to ensure uniform exposure and adequate airflow (Figure 1D).

D-limonene solutions were prepared from cold-pressed citrus peel essential oil (ProLyks Natural, Hydroplan-EB®®), which contains 58% *Citrus* × *sinensis* (L.) Osbeck essential oil. This product is IBD-certified and approved for organic agriculture in accordance with international and national standards (NOP/USA, IBD/IFOAM, COR/Canada, and Brazilian Law 10.831/2003). Each solution was diluted in deionized water, which was also used for the control treatment (0.00 $mL \cdot L^{-1}$). Applications were performed weekly by using a manual sprayer with a conical tip (Stihl SG 11®®; v = 1.5 L; pressure = 3.0 bar; Q = 0.6 $L \cdot min^{-1}$), starting on October 7 and continuing until November 25, 2024. Initially, 100 mL of solution was applied per pot, with the volume gradually adjusted to ensure complete coverage of the leaf surface as plants developed, avoiding runoff.

2.3. Biometric and Biomass Measurements

Biometric evaluations were conducted weekly from October 4 to November 29, 2024, spanning a period of 2 to 60 DAT. Plant height was measured from the substrate surface to the apical meristem using a 10 meter fiberglass measuring tape. Stem diameter was measured at the base of the main stem using a digital caliper (Digimess®®, model 100.174BL). The number of leaves was also recorded at 7-day intervals, while secondary shoot counts began at 30 DAT and continued weekly thereafter. For all non-destructive biometric variables, the values used in the statistical analysis correspond to the mean of all evaluation periods throughout the experimental timeline (4 evaluation periods for the number of secondary shoots and 9 for the other variables).

At the end of the experiment, all plants were harvested and separated into roots, stems, and leaves. The plant material was dried in a forced-ventilation circulation oven at 65 ± 1 °C until reaching constant weight. Dry matter was determined individually for roots, stems, and leaves using an

 doi:10.20944/preprints202506.1461.v1

analytical balance (Shimadzu®®, model AY220; precision 0.01 g). This data was used to calculate total shoot and root dry matter.

2.4. Photosynthetic Pigments and Bioactive Compounds Analysis

For the analysis of photosynthetic pigments, a total of 10 g of fresh leaf tissue was collected on November 29, 2024, the final day of evaluation. Samples were obtained from the apical, median, and basal regions of each plant to ensure representativeness. Chlorophyll *a*, chlorophyll *b*, and total chlorophyll were quantified using fresh macerated tissue, following the method described by Hiscox and Israelstam (1979) [28]. From each composite sample, 50 mg of fresh tissue was weighed using an analytical balance (Shimadzu®®, model UX420H; precision 0.001 g), homogenized in 5 mL of dimethyl sulfoxide, and incubated at 25 ± 5 °C for 48 hours in the dark. After extraction, the solution was used for spectrophotometric analysis (Bel, model V-M5) at wavelengths of 665 and 649 nm. Thus, pigment concentrations were calculated using specific equations and expressed in g·kg^{-1} of fresh biomass. All procedures were carried out in triplicate to ensure analytical reliability:

$$Chlorophyll\ a = \frac{[(12.9 \times A_{665}) - (3.45 \times A_{649})] \times \left(\frac{\text{dilution factor}}{1.1}\right)}{1000} \quad (1)$$

$$Chlorophyll\ b = \frac{[(21.99 \times A_{649}) - (5.32 \times A_{665})] \times \left(\frac{\text{dilution factor}}{1.1}\right)}{1000} \quad (2)$$

$$Total\ chlorophyll = Chlorophyll\ a + Chlorophyll\ b \quad (3)$$

For the analysis of bioactive compounds, leaf samples were also collected on November 29, 2024, from the apical, median, and basal regions of each plant. After collecting, approximately 10 g of fresh leaves per treatment were oven-dried in a forced-air circulation oven at 65 °C for 72 hours. The dried material was then ground using a Willey-type mill (Marconi®®, model MA-048) equipped with a 0.5 mm sieve.

Total Anthocyanins and flavonoids contents were determined by spectrophotometry using methods adapted from Lees and Francis (1972) [29] and Siegelman and Hendricks (1958) [30]. For each determination, 50 mg of dried and ground leaf material was weighed using an analytical balance (Shimadzu®®, model UX420H; precision 0.001 g) and extracted in 10 mL of 1% HCl in 80% methanol. The samples were incubated in the dark at 4 °C for 12 hours. An aliquot of the extract was then collected, and absorbance was measured at 530 and 350 nm using a spectrophotometer (Bel, model V-M5). These measurements were also performed in triplicate. Results were expressed in g·kg^{-1} of dry mass using the appropriate equations:

$$Total\ anthocyanins = \frac{A_{530} \times \text{dilution factor}}{98.2} \quad (4)$$

$$Total\ flavonoids = \frac{A_{350} \times \text{dilution factor}}{76.5} \quad (5)$$

Coumarin content was analyzed at the Research Laboratory of Apis Flora in Ribeirão Preto-SP, Brazil (Figure 1A, B), using high-performance liquid chromatography (HPLC) as described by Medeiros et al. (2010) [31]. For extraction, dry leaf samples were prepared at a concentration of 50 mg·mL^{-1} in a 1:1 (v/v) mixture of HPLC-grade methanol and ultrapure water, followed by ultrasonic treatment for 60 minutes. The extract was filtered through cotton into a volumetric flask, and the remaining material was subjected to a second extraction under identical conditions for 15 minutes. Both extracts were combined, filtered, and passed through a 0.45 µm membrane filter prior to injection.

Chromatographic separation was carried out on a Shimadzu HPLC system equipped with an SPD-M20A photodiode array detector and a Shim-Pack CLC-ODS column (4.6 × 250 mm, 5 µm, 100 Å). The mobile phase consisted of a methanol–ultrapure water gradient ranging from 35% to 95% over 24 minutes, at a constant flow rate of 1.0 mL·min^{-1}. The injection volume was 20 µL, with the column maintained at 40 °C. Detection was performed at 275 nm, and coumarin was identified by its retention time (~12.3 minutes). Quantification was based on a calibration curve constructed with

 doi:10.20944/preprints202506.1461.v1

standard solutions between 20 and 100 μg·mL^{-1}. The entire chromatographic procedure was replicated three times.

2.5. Statistical Analysis

The original data were initially tested for normal distribution using the Shapiro–Wilk and Kolmogorov–Smirnov tests, and for homogeneity of variances using Bartlett's test, all at the 5% significance level. When necessary, data were subjected to appropriate transformations to meet the assumptions of normality and homoscedasticity. Subsequently, analysis of variance (ANOVA) was performed using the F-test at the 5% significance level. For statistically significant effects or interactions, qualitative factors (colored shade nets) were compared using Tukey's test ($p \leq 0.05$), while quantitative variables (D-limonene doses) were analyzed by regression analysis. In cases of significant interaction between main plots and subplots, regression analysis was performed within each light condition. All statistical procedures were carried out using Assistat Software®® (Version 7.7) [32], and graphical outputs were produced with SigmaPlot®® (Version 16.0).

3. Results

3.1. Biometric and Biomass Measurements

The analysis of variance demonstrated that the biometric variables of *M. laevigata* were significantly influenced ($p < 0.05$) by the different colored shade nets, with notable effects observed for plant height, number of leaves, leaf dry matter, shoot dry matter, root dry matter and number of secondary shoots. D-limonene doses also had a significant effect on all biometric traits evaluated. Significant interaction between these two factors ($p < 0.01$ to $p < 0.05$) was also detected for plant height, stem diameter, number of leaves and leaf dry matter. Moreover, all biometric variables showed a normal distribution according to the Shapiro–Wilk test at the 5% significance level, except for leaf dry matter and plant height, which met the normality assumption based on the Kolmogorov–Smirnov also at 5%. Detailed mean square values and coefficients of variation for these attributes are presented in Table 2.

Table 2. Summary of the analysis of variance for plant height (PH), plant diameter (PD), number of leaves (NL), shoot dry matter (SDM), leaves dry matter (LDM), root dry matter (RDM), and number of secondary shoots (SSN) of *M. laevigata* plants grown under four light conditions (colored shade nets compared to full sunlight) and five D-limonene doses.

Source of Variation	Mean Square							
	DF	PH	PD	NL	SSN	LDM	SDM	RDM
Colored shade nets (A)	3	6956.10**	0.33^{ns}	211.71**	3.91**	2452.96**	7180.34**	3125.33**
D-limonene dose (B)	4	1075.12**	8.51**	599.19**	282.10**	223.70**	842.29**	459.00**
A x B Interaction	12	91.60**	0.05*	33.26**	1.47^{ns}	9.63**	32.28^{ns}	3.66^{ns}
Linear Regression (B)	1	—	—	—	1108.59**	—	406.50**	2.00^{ns}
Quadratic Regression (B)	1	—	—	—	0.21^{ns}	—	100.65**	1555.71**
Residual (A)	64	4.93	0.18	17.19	0.53	6.95	27.30	4.97
Residual (B)	64	6.10	0.02	5.94	0.94	1.78	28.46	6.34
CV (%)		14.59	12.83	12.66	44.33	30.34	31.43	39.83
p-value (A x B)		< 0.0001	0.0429	< 0.0001	0.1259	< 0.0001	0.3495	0.8525

Note: The variables plant height, stem diameter, number of leaves and secondary shoot number represent the average values across all measurement periods. The symbol "—" indicates that regression analysis was performed within each light condition (colored shade nets and full sunlight) due to a significant interaction between factors (A × B); "ns" denotes non-significant effects at $p \geq 0.05$; * indicates significance at $p < 0.05$; ** indicates significance at $p < 0.01$; degrees of freedom (DF); coefficient of variation (CV).

Plant height in *M. laevigata* responded significantly to D-limonene doses across all light conditions, exhibiting a quadratic pattern (Figure 2A). Due to the statistical interaction between these factors, regression analysis was conducted within each shade condition and was significant at the 1% level ($p < 0.01$) for all cases. The fitted regression models yielded coefficients of determination (R^2) ranging from 0.76 to 0.92, indicating a reasonable fit between the estimated curves and the observed data. The maximum plant height was recorded under the red shade net, reaching 141.59 cm at an optimal D-limonene concentration of 0.98 mL L^{-1}, followed by the black net (129.50 cm at 1.21 mL L^{-1}), blue net (116.57 cm at 1.22 mL L^{-1}), and full sunlight (102.63 cm at 1.14 mL L^{-1}). This consistent ranking (red > black > blue > full sunlight) was statistically supported across all experimental

 doi:10.20944/preprints202506.1461.v1

environments. Overall, plant height consistently increased with D-limonene application up to intermediate doses (1.00–1.20 mL L^{-1}) and subsequently declined at the highest concentration (2.00 mL L^{-1}), thereby confirming the quadratic nature of the dose response to this terpenoid.

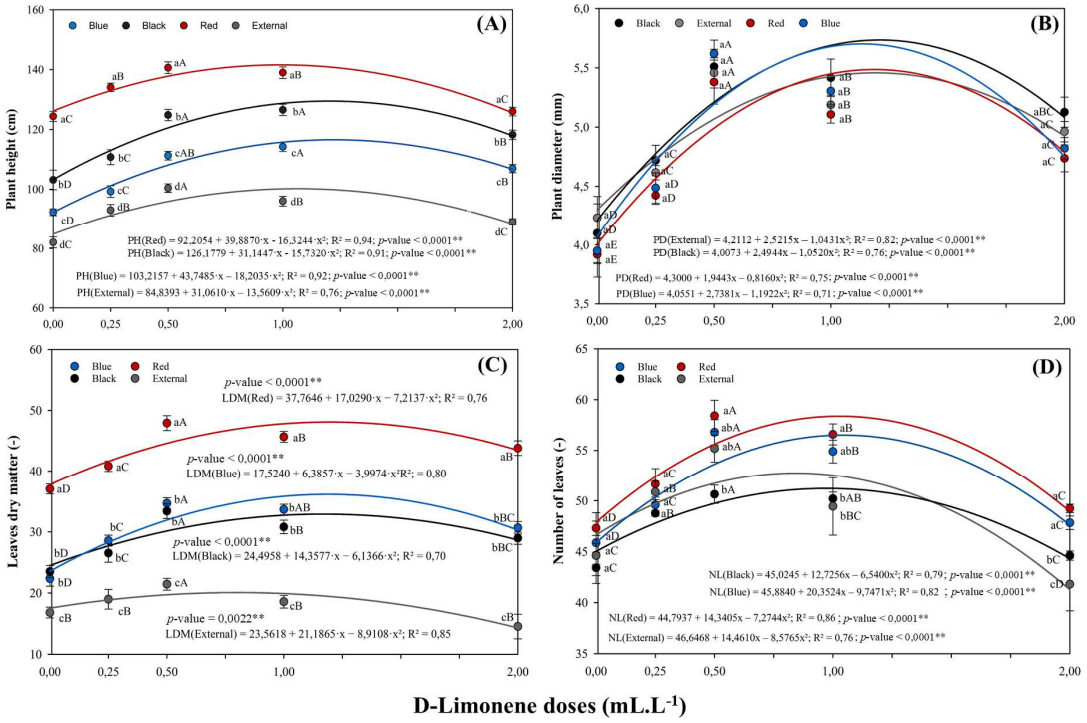

Figure 2. Plant height (A), stem diameter (B), leaves dry matter (C), and number of leaves (D) in *M. laevigata* in response to D-limonene foliar application under different light conditions. Values represent the mean ± standard error. Different lowercase letters compare means among D-limonene doses within each shade condition, while uppercase letters compare light conditions at the same dose. ** The regression analysis for D-limonene doses was significant for quadratic terms at 1% significance ($p < 0.01$).

On the other hand, stem diameter was not significantly affected by the light environment but showed a significant response to D-limonene doses, also following a quadratic pattern (Figure 2B). Given the observed interaction between the factors, separate regression analyses were performed for each shading condition, all of which exhibited a significant quadratic trend at the 1% probability level ($p < 0.01$). Stem diameter consistently increased with rising D-limonene concentrations up to intermediate levels, similar to the pattern observed for plant height, before declining at the highest dose assessed. Although no statistical differences were detected among light conditions, the fitted quadratic regression models indicated superior responses for stem diameter under the black and blue shade nets. The estimated maximum values for these conditions were 5.73 mm and 5.62 mm, respectively, achieved at optimal doses between 1.14 and 1.20 mL L^{-1}. In contrast, the curves fitted for the red net and full sunlight displayed more modest peaks, yielding maximum diameters of 5.49 mm and 5.46 mm, respectively, at an optimal concentration of 1.18 mL L^{-1}.

Leaves dry matter were significantly affected by the interaction between light environment and D-limonene dose, with a quadratic regression model effectively fitted for each light condition ($p < 0.01$). Regression analyses indicated that the highest estimated foliar biomass was obtained under the red shade net, reaching 47.81 g $plant^{-1}$ at an optimal dose of 1.18 mL L^{-1} (Figure 2C). The blue and black nets yielded intermediate values, with estimated peaks of 36.16 g and 32.89 g, respectively, both occurring at concentrations approximating 1.18 mL L^{-1}. While these two conditions did not statistically differ from each other, both produced significantly lower biomass compared to the red net. The lowest performance at the optimal dose was observed under full sunlight, yielding a maximum estimated value of 20.07 g at 0.80 mL L^{-1}.

In this context, the number of leaves was also affected by both light conditions and D-limonene application, exhibiting a significant interaction between the factors (Figure 2D). Quadratic regression

 doi:10.20944/preprints202506.1461.v1

models were successfully fitted for each light condition, with all models proving significant at the 1% probability level ($p < 0.01$) and yielding R^2 ranging from 0.76 to 0.86. The highest estimated value was observed under the red shade net, reaching 56.17 leaves per plant at a concentration of 1.19 mL L^{-1}. The blue net yielded 53.60 leaves, while full sunlight peaked at 51.21 leaves, both at optimal doses approximating 1.21 mL L^{-1}. In contrast, the black net exhibited the lowest maximum value, with 47.64 leaves at 1.23 mL L^{-1}. Post-hoc analysis using Tukey's test ($p < 0.05$) revealed that the red net significantly differed from all other light environments. Furthermore, the blue and full sunlight conditions were statistically equivalent and superior to the black net.

Thereafter, the number of secondary shoots was significantly influenced by both D-limonene doses and light conditions, although no interaction was observed between these factors (Figure 3A, B). A general regression analysis was applied to assess the dose–response pattern, revealing a significant linear effect ($p < 0.01$) with R^2 of 0.90. This analysis indicated that the highest value for this parameter was recorded at the maximum applied dose (2.00 mL L^{-1}), yielding an average of 12.85 shoots per plant. This represents a substantial increase of approximately 360% compared to the control treatment (2.81 shoots at 0.00 mL L^{-1}). Regarding light conditions, plants cultivated under full sunlight exhibited the highest average number of secondary shoots (8.40 shoots $plant^{-1}$), significantly differing from all other tested conditions. The red (7.90 shoots) and black (7.43 shoots) shade nets yielded intermediate values and did not statistically differ from each other. In contrast, the blue net presented the lowest average (7.23 shoots) and was statistically inferior to full sunlight, indicating a reduced potential for axillary shoot development within this specific light environment.

Within biomass production, both the shoot and root dry matter of *M. laevigata* were significantly affected by light conditions and D-limonene doses, although no significant interaction was observed between these factors. A separate regression analysis, conducted for each variable, revealed a significant quadratic response ($p < 0.01$). The models showed good statistical fits, with R^2 of 0.79 for shoot dry matter and 0.85 for root dry matter. For shoot dry matter (Figures 3C, D), the highest estimated value was 59.18 g per plant, achieved at a D-limonene dose of 1.08 mL L^{-1}. This represented an increase of approximately 27.2% compared to the control group (46.54 g at 0.00 mL L^{-1}). Among the light conditions, the red shade net consistently promoted the greatest accumulation of shoot biomass (76.96 g). This yield was statistically superior to that observed under both the black (61.11 g) and blue (53.52 g) nets, which, notably, did not statistically differ from each other. The full sunlight condition resulted in the lowest shoot biomass (30.86 g), marking a reduction of nearly 59.9% relative to the red net. Conversely, for root dry matter (Figures 3E, F), the regression model indicated a peak value of 33.27 g per plant at a dose of 0.93 mL L^{-1}, while the control treatment averaged 24.57 g, a gain of 35.4%. Regarding the effect of light, the black shade net yielded the highest root mass (40.00 g), followed by the red (31.20 g) and blue nets (24.00 g), which formed a statistically intermediate group. Consistently, the lowest value was recorded under full sunlight (13.60 g), further confirming that unfiltered light significantly limited belowground biomass development.

 doi:10.20944/preprints202506.1461.v1

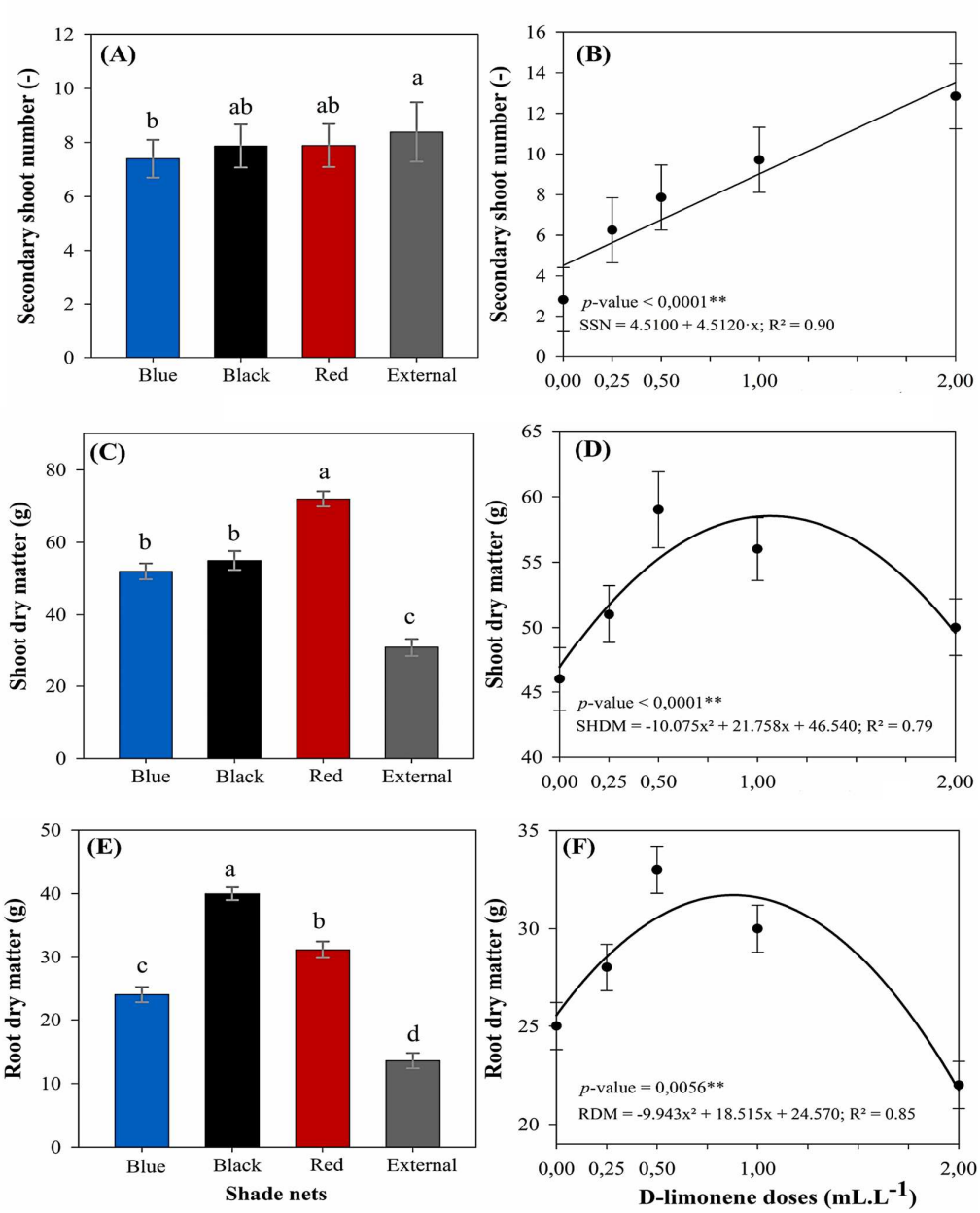

Figure 3. Secondary shoot number (A, B), shoot dry matter (C, D), and root dry matter (E, F) in *M. laevigata* in response to D-limonene doses and light conditions. Values represent the mean ± standard error. Different lowercase letters indicate significant differences according to Tukey's test ($p < 0.05$). ** The regression analysis for D-limonene doses was significant for linear (B) and quadratic terms (D, F) at 1% significance ($p < 0.01$).

3.2. *Photosynthetic Pigments and Bioactive Compounds Analysis*

The analysis of variance demonstrated that both photosynthetic pigments and pharmacological compounds were significantly influenced by the light environment. For the pigment variables, significant effects ($p < 0.05$ to $p < 0.01$) were observed for chlorophyll *a*, chlorophyll *b*, and total chlorophyll. Similarly, the concentrations of anthocyanins, flavonoids, coumarins, and the coumarin-to-total-chlorophyll ratio were also affected by light conditions ($p < 0.01$). In contrast, D-limonene doses did not significantly influence any of these traits, and no interaction between light environment and D-limonene application was detected for any variable.

All photosynthetic pigment variables followed a normal distribution according to the Shapiro–Wilk test at the 5% significance level, with the exception of the chlorophyll *a*/*b* ratio, which required

 doi:10.20944/preprints202506.1461.v1

logarithmic transformation to satisfy the assumptions of normality. For pharmacological compounds, flavonoid data met the normality assumption directly, while anthocyanins, coumarins, and the coumarin-to-chlorophyll ratio achieved normality after Box-Cox transformation, confirmed by the Kolmogorov–Smirnov test at the same significance level. Detailed mean square values and coefficients of variation for all secondary metabolite traits are presented in Table 3.

Table 3. Summary of the analysis of variance for chlorophyll pigments and bioactive compounds in *M. laevigata* under four light environments and five D-limonene doses.

Source of Variation	Mean Square								
	DF	Chl *a*	Chl *b*	ChlT	Chl *a*/*b*	Anth	Flav	Cum	Cum/ChlT
Colored shade nets (A)	3	16642.16**	6186.35**	42312.49**	0.04619*	0.00977**	3.23**	17.33**	413.94**
D-limonene dose (B)	4	871.08^{ns}	363.21^{ns}	1915.52^{ns}	0.00645^{ns}	0.00005^{ns}	0.19^{ns}	0.09^{ns}	5.45^{ns}
A x B Interaction	12	386.00^{ns}	452.46^{ns}	711.96^{ns}	0.01424^{ns}	0.00002^{ns}	0.25^{ns}	0.04^{ns}	3.30^{ns}
Quadratic Regression (B)	1	ns	ns	ns	ns	ns	Ns	ns	ns
Residual (A)	64	464.63	363.21	887.12	0.01124	0.00003	0.17202	0.046	3.00
Residual (B)	64	534.27	361.21	864.48	0.01515	0.00003	0.11569	0.053	2.56
CV (%)		14.95	27.79	15.63	29.33	30.20	19.01	13.48	19.98
p-value (A x B)		0.7242	0.2687	0.6258	0.5140	0.7245	0.2650	0.7242	0.2649

Note: Chlorophyll *a*/*b* is a calculated index derived from respective pigment concentrations. ns: non-significant at $p \geq 0.05$; *: significant at $p < 0.05$; **: significant at $p < 0.01$; degrees of freedom (DF); coefficient of variation (CV); chlorophyll *a* (Chl *a*); chlorophyll *b* (Chl *b*); total chlorophyll (ChlT); chlorophyll *a*/*b* ratio (Chl *a*/*b*); anthocyanins (Anth); flavonoids (Flav); coumarins (Cum); and coumarin-to-chlorophyll ratio (Cum/ChlT).

In relation to chlorophyll *a* content (Figure 4A), plants grown under the blue shade net exhibited the highest concentration (237.65 μg g^{-1}), which significantly surpassed all other light environments. The red (212.81 μg g^{-1}) and black (218.23 μg g^{-1}) nets yielded intermediate values, showing no statistical difference between them. Full sunlight exposure resulted in the lowest value (175.91 μg g^{-1}), representing a substantial decrease of approximately 35% when compared to blue net conditions. A similar pattern was observed for chlorophyll *b* (Figure 4B). The blue net again yielded the highest concentration (96.46 μg g^{-1}), although it was not statistically different from the red (91.09 μg g^{-1}) and black (86.58 μg g^{-1}) nets. In contrast, full sunlight exposition resulted in the lowest mean (61.02 μg g^{-1}). Total chlorophyll content (Figure 4C) followed a similar trend, with the blue net promoting the highest accumulation (334.12 μg g^{-1}), significantly higher than all other treatments. The red (303.91 μg g^{-1}) and black (304.82 μg g^{-1}) nets formed a statistically indistinguishable group, whereas full sunlight yielded the lowest pigment concentration (236.94 μg g^{-1}). The chlorophyll *a*/*b* ratio (Figure 4D) displayed an inverse behavior. The highest ratio was recorded under full sunlight (3.17), significantly greater than values observed under the black (2.49 μg g^{-1}) and red (2.62) nets. The blue net yielded the lowest ratio (2.56), which was statistically similar to the red and black treatments but significantly lower than that under full sunlight.

Anthocyanin content (Figure 4E) was highest under full sunlight (0.084 μg·g^{-1}), significantly surpassing all other light environments. The lowest value was recorded under the blue net (0.036 μg·g^{-1}), representing a reduction of over 57% relative to full sunlight. The red shade net yielded an intermediate concentration of 0.054 μg·g^{-1}, which, despite being numerically higher than the black net, did not statistically differ from it. Therefore, both the red and black nets formed a statistical group with intermediate anthocyanin levels. For flavonoids (Figure 4F), the red and external environment exhibited the highest and statistically similar concentrations (2.78 and 2.71 mg·g^{-1}, respectively). In contrast, the black net resulted in the lowest value (2.02 mg·g^{-1}), which was significantly different from the other light treatments. This represented a 27% decrease in flavonoid content compared to the red net.

 doi:10.20944/preprints202506.1461.v1

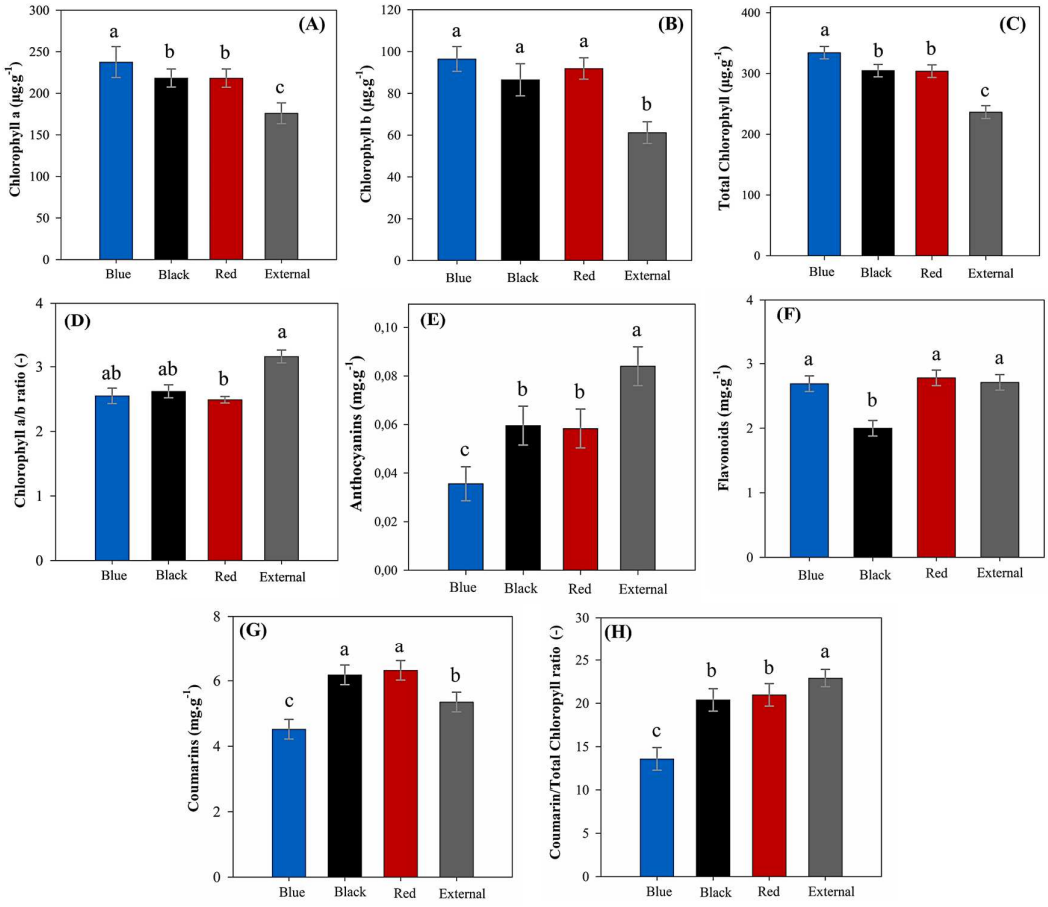

Figure 4. Content of photosynthetic pigments and bioactive compounds in leaves of *M. laevigata* under different light conditions. Bars represent the mean ± standard error. Different lowercase letters indicate significant differences among light conditions according to Tukey's test ($p < 0.05$). (A) Chlorophyll *a* content, (B) Chlorophyll *b* content, (C) Total chlorophyll content, (D) Chlorophyll *a/b* ratio, (E) Anthocyanin content, (F) Flavonoid content, (G) Coumarin content, and (H) Coumarin/Total chlorophyll ratio.

Similarly, coumarin content (Figure 4G) was favored by red (6.33 mg·g^{-1}) and black (6.18 mg·g^{-1}) nets, which did not differ statistically, whereas the blue net showed the lowest value (4.53 mg·g^{-1}), representing a 28.5% reduction compared to the red net. Furthermore, compared to the control treatment in full sun (5.36 mg·g^{-1}), the red and black nets led to coumarin content increases of approximately 18.1% and 15.4%, respectively. Regarding the coumarin-to-total-chlorophyll ratio (Figure 4H), full sunlight exhibited the highest proportion (22.93), significantly greater than observed under the black (20.40) and red (20.99) nets, which were statistically similar. The blue net showed the lowest ratio (13.59), nearly 41% lower than the full sunlight.

4. Discussion

4.1. Biometric and Biomass Measurements

Among microclimatic factors assessed, global solar radiation exhibited the highest divergence across treatments (Figure 5), thereby underscoring the capacity of colored shade nets to alter both the quantity and quality of incident light. Compared to the control treatment (full sunlight), the blue net reduced light transmission to 20.5%, while the red and black nets allowed 38.9% and 32.3%, respectively, with no statistical difference detected between them. These findings align with those reported by Honorato et al. (2023) [33], who similarly observed the lowest solar radiation transmittance under blue nets and intermediate levels under red and black nets.

 doi:10.20944/preprints202506.1461.v1

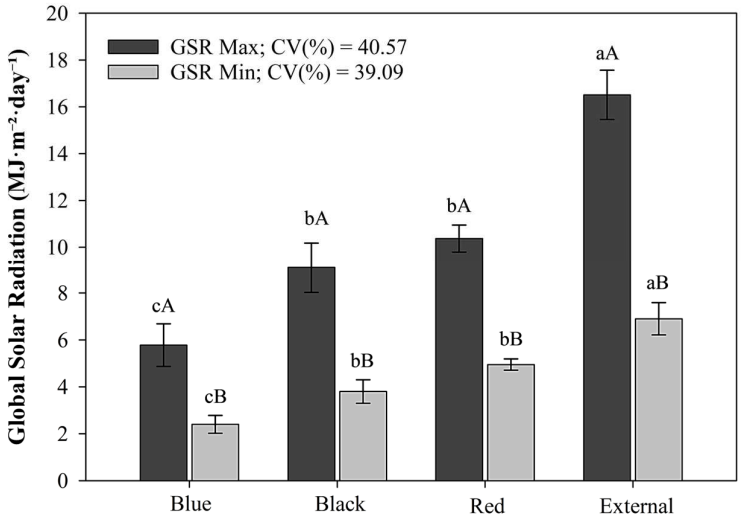

Figure 5. Average maximum and minimum daily global solar radiation under the colored shade nets and full sunlight (external environment), recorded from October 2 to November 29, 2024. Values represent the mean ± standard error. Bars with the same lowercase letters (within each environment) and uppercase letters (between environments) do not differ by Tukey's test ($p \leq 0.05$). Coefficient of variation (CV).

Although ChromatiNET®® nets are commercially marketed with a nominal 50% shading efficiency, the actual transmissivity measured in this study was notably lower, indicating a clear discrepancy between manufacturer specifications and field performance. This observation has also been reported in other studies, which demonstrate that colored shade nets not only modify light spectrum, but also alter other environmental conditions, including air temperature, relative humidity, airflow, and overall radiation levels [34–36].

Despite these microclimatic shifts, other environmental parameters remained relatively stable across treatments (Table 1). This suggests that light intensity and its spectral composition were the primary drivers of the observed plant responses in this study [37–39]. In this context, the reduced plant growth under full sunlight conditions likely resulted from photoinhibition due to excessive light availability, whereas the limited light under the blue net likely led to insufficient photosynthetic stimulation (Figures 2 and 3). This interpretation is further corroborated by the pattern of anthocyanin accumulation (Figure 4E), which was highest under full sunlight and lowest under the blue net, thereby indicating varying degrees of light-induced stress [40,41]. Thus, these findings align with those of Contin et al. (2021) [19], who reported increased growth of *M. laevigata* cultivated under moderate shading (25-50%).

Additionally, the significantly greater plant height under the red net compared to the black net suggests that the light spectrum, particularly the red-to-far-red (R/FR) ratio, may have played a more pronounced effect on shoot elongation (Figure 2A). From this perspective, Han et al. (2024) [42] demonstrated that changes in R/FR ratios influence phytochrome-mediated signaling, leading to enhanced gibberellin biosynthesis and internode elongation [41,43]. While this finding contrasts with Souza et al. (2011) [22], who reported greater height in *M. glomerata* grown under blue nets, it is consistent with observations by Harish et al. (2022) [44] in *Curcuma longa* L. and Zhang et al. (2022) [45] in *Camellia sinensis* (L.) Kuntze, both studies having reported increased vertical growth under red netting.

In contrast, the stem diameter did not differ significantly among light conditions (Figure 2B), reflecting similar findings by Souza et al. (2010) [17] and Souza et al. (2011) [22], who also reported no changes in this parameter for *M. glomerata* cultivated under colored shade nets. These results suggest that, in shade-adapted species, stem thickening is less sensitive to variations in light intensity and spectral quality, whereas shoot elongation appears more responsive to such environmental cues, likely due to etiolation processes. Similar responses have been observed in *Physalis peruviana* L. [46] and *Ocimum selloi* Benth. [47], reinforcing the hypotheses that under shaded conditions, morphological plasticity is more pronounced in vertical growth than in radial expansion.

Subsequently, the results regarding leaf number per plant (Figure 2D) also appear to align with Harish et al. (2022) [44], who observed enhanced vegetative performance under red and blue shade

 doi:10.20944/preprints202506.1461.v1

nets when compared to full sunlight. According to Ilić et al. (2017) [48], the greater leaf production under the red net may be attributed to a higher photosynthetic photon flux density (PPFD), particularly in the red and far-red regions, which could stimulate cell division and meristematic development [49]. From this perspective, blue nets might also influence leaf formation by modulating photomorphogenic pathways through the activation of cryptochromes and phototropins [50]. In contrast, the limited spectral selectivity of the black net, coupled with potential stress under full sunlight, likely restricted overall vegetative growth and suppressed leaf emergence [19,33,44].

Contrary to our initial expectations, the number of secondary shoots varied significantly across the colored shade nets (Figure 3A). The distribution of this morphologic variable is closely related to the gradient of solar radiation among light conditions, suggesting that solar radiation intensity likely played a central role in regulating lateral shoot formation. One possible explanation for this phenomenon involves the dynamic behavior of auxin, a hormone that maintains apical dominance by suppressing axillary bud growth [51]. Under high irradiance, auxins are more susceptible to photodegradation, which can reduce their inhibitory effect and thereby promote increased branching [23,52].

Beyond morphological traits, biomass accumulation provided additional insights into the effects of colored shade nets on *M. laevigata* growth. In this study, shoot dry mass closely followed the trend observed for leaf dry matter, with the highest values under the red net (Figure 3C). These results contrast with those of Souza et al. (2011) [17] and Ribeiro et al. (2024) [54], who reported greater aboveground biomass under blue netting for *Mikania glomerata* Spreng. and *Lippia dulcis* Trevir., respectively. Otherwise, the present findings are consistent with Ribeiro et al. (2018) [55], who observed a similar pattern in *Pogostemon cablin* (Blanco) Benth., with the red net promoting the highest yields, followed by the black net, blue net, and full sunlight.

Conversely, in the present experiment, root dry matter was highest under the black net (Figure 3E), which contrasts with previous studies, including Souza et al. (2011) [22], who reported increased root biomass of *M. glomerata* under blue and red nets, as well as similar trends in other medicinal species [17,33,44,55]. Although the black and red nets transmitted comparable levels of solar radiation (Figure 5), only the red net significantly modified the spectral composition by enriching red and far-red wavelengths, which are known to promote shoot elongation and suppress root development [47,54]. In contrast, the absence of spectral enrichment under the black net may have limited shoot stimulation and led to a preferential allocation of assimilates to the roots, favoring belowground growth as an adaptive response to specifics light and thermal conditions.

In addition to the morphological responses promoted by the colored shade nets, this study revealed that *M. laevigata* responded significantly to D-limonene in a dose-dependent manner (Figures 2 and 3). Most biometric traits exhibited a quadratic pattern, characterized by increases up to approximately 1.20 $mL \cdot L^{-1}$, followed by reductions at higher concentrations, indicative of a typical hormetic response [56,57]. In contrast, the number of secondary shoots increased linearly with dosage. This behavior, in which low concentrations stimulate plant development and higher suppress it, has been widely documented for various bioactive compounds, including bioherbicides, allelochemicals and other terpenoids [58,59]. Extending this, a plausible explanation for the observed growth response is proposed by Lin et al. (2024) [60], who reported that D-limonene may influence key metabolic pathways related to energy production (glycolysis, Krebs cycle, and oxidative phosphorylation), potentially increasing ATP availability and supporting cell expansion and division. Furthermore, Ninkuu et al. (2021) [61] demonstrate that monoterpenes can interact with hormonal pathways and intracellular signaling mechanisms, modulating plant development in a concentration-dependent manner. These combined mechanisms may help explain the biomass and morphological development gains observed at lower D-limonene concentrations. Similarly, Hassan et al. (2016) [62] and Pannacci et al. (2022) [57] reported hormetic effects, with increased root and shoot biomass at low concentrations and inhibition at higher levels, following the foliar application of other bioactive compounds.

In contrast, the inhibitory effects observed at higher D-limonene concentrations suggest a shift from physiological stimulation to phytotoxicity [63,64], as evidenced by the decline in biomass accumulation and morphological development from the 1.20 $mL \cdot L^{-1}$ dose onward. This trend is consistent with findings by Gettys et al. (2023) [63], who reported biomass reductions exceeding 90% in *Pistia stratiotes* L. treated with 20–30% of D-limonene. Similarly, Sbagui and Alaloui (2025) [64] observed severe tissue degradation and turgor loss in plants exposed to high concentrations of this terpenoid. Furthermore, according to Lin et al. (2024) [60], D-limonene compromises the integrity of cell

 doi:10.20944/preprints202506.1461.v1

membranes and walls by increasing permeability and disturbing ion homeostasis [65,66], which may also underline the physiological stress and growth suppression observed in *M. laevigata.*

In this regard, the linear increase in the number of secondary shoots (Figure 3B) may reflect a stress-induced developmental response resulting from the degradation of cell membranes caused by D-limonene [60,65,66], considering that meristematic tissues are particularly sensitive to structural disruptions [51]. Furthermore, such damage may interfere with cell division and hormonal regulation, potentially leading to altered shoot initiation as a compensatory mechanism under stress conditions [61]. To some extent, this observation is also consistent with the hormetic effect described for the other biometric variables, as it suggests a shift in developmental patterns in response to increasing doses of D-limonene, reinforcing the dose-dependent duality between stimulation and inhibition.

4.2. Photosynthetic Pigments and Bioactive Compounds

Photosynthetic pigment levels are widely recognized as reliable indicators of photosynthetic performance, given their central role in light absorption and energy conversion, which directly influence plant development and adaptation to environmental conditions [48,51]. In the present research, the absence of significant changes in chlorophyll content following foliar D-limonene application suggests that this monoterpene does not exert its effects through direct modulation of the photosynthetic apparatus of *M. laevigata*. This finding is consistent with the previously proposed hypothesis, that the biostimulatory responses observed for this terpenoid are likely mediated by post-photosynthetic metabolic pathways, potentially involving enhanced efficiency in photoassimilate utilization and the regulation of hormonal signaling [60,61].

In contrast to the absence of a response to D-limonene, variations in pigment content were observed across the photoselective shade nets. In this experiment, total chlorophyll and chlorophyll *a* exhibited a distribution pattern aligned with global solar radiation levels, with higher concentrations under the blue net and lower values under full sunlight (Figure 4A, C). This suggests a predominant role of light intensity in their accumulation [20,34–36]. According to Honorato et al. (2023) [33], increased pigment content under shading likely reflects an adaptive response to enhance the capture of diffuse radiation, thereby improving carbohydrate production and supporting plant growth under conditions of reduced irradiance. Similar results were reported by Ilić et al. (2017) [48] and Harish et al. (2022) [44], who also found higher chlorophyll levels in leaves under colored nets compared to external environments, further reinforcing the influence of light intensity on pigment accumulation.

In this context, the greater accumulation of total chlorophyll and chlorophyll *a* under the blue shade net aligns with the findings of Souza et al. (2011) [22]. The authors reported higher levels of these pigments under blue nets and the lowest under full sunlight for *M. glomerata*. Consistent with this, Contin et al. (2020) observed reduced chlorophyll content in this species cultivated under full sunlight compared to shaded conditions. However, the present experiment found no significant differences in chlorophyll *b* among the colored nets (Figure 4B). This may be attributed to the saturation of chlorophyll *b* synthesis under moderate shading, beyond which additional changes in light quantity do not affect its accumulation [51]. A similar result was reported by Díaz-Pérez and John (2019) [67], who also observed uniform chlorophyll *b* levels across colored shade nets.

Furthermore, higher chlorophyll *a/b* ratios were observed under the external environment, while lower values occurred under shaded conditions, particularly beneath the red net (Figure 4D). This pattern likely reflects a photomorphogenic adjustment, in which plants exposed to high irradiance reduce chlorophyll *b* content to mitigate excessive light absorption, whereas those under lower irradiance increase their proportion to enhance light capture through larger antenna complexes [28,33,51]. Thus, although the red and black nets provided comparable irradiance levels, the red net resulted in lower *a/b* ratios, possibly due to its distinct red to far-red light ratio, a spectral feature known to regulate pigment synthesis and allocation [42,44,51]. Nevertheless, this outcome contrasts with the findings of Souza et al. (2011) [22], who reported no significant differences in the *a/b* ratio of *M. glomerata* and *M. laevigata* cultivated under different colored shade nets.

Similarly, a positive correlation was observed between light quantity and anthocyanin synthesis (Figure 4E), suggesting an adaptive role of these pigments as part of a response to potential light-induced stress [40,41]. Given the well-recognized photoprotective function of anthocyanins in safeguarding the photosynthetic apparatus, their higher accumulation in leaves under full sunlight conditions may be associated with increased radiation exposure, which could lead to greater production of reactive oxygen species and, consequently, induce antioxidant responses [51]. This hypothesis is

 doi:10.20944/preprints202506.1461.v1

supported by Zoratti et al. (2015) [68], who reported greater anthocyanin accumulation in *Vaccinium corymbosum* L. under high irradiance. Furthermore, Wolske et al. (2021) [69] observed significant reductions in these compounds in *Ribes nigrum* L. subjected to artificial shading.

Conversely, the flavonoid content observed in *M. laevigata* leaves in the present study (Figure 4F) contrasts with findings reported by several authors, who observed significant reductions in these compounds under shading compared to full sunlight [70–74]. Although flavonoids are well known for their photoprotective and antioxidant functions [51], it is likely that their distribution across light environments was not solely influenced by irradiance, but also by the spectral quality of light. In support of this interpretation, Fu et al. (2016) [75] demonstrated that light spectra enriched in blue and far-red wavelengths can enhance flavonoid biosynthesis, even under low light intensity, through the activation of photoreceptors and the upregulation of specific genes.

Expanding on this, Ye et al. (2021) [71] also reported that spectral modulation can influence the phenylpropanoid pathway in *C. sinensis* leaves, even under shaded conditions. Accordingly, the elevated flavonoid levels observed under the blue net in the present study may be associated with the enrichment of blue wavelengths, which are known to stimulate this metabolic route. In contrast, the accumulation of flavonoids under full sunlight is probably related to increased photoprotective demand in response to high irradiance. The lower concentrations detected under the black net, by comparison, may reflect the combined effects of reduced light intensity and the absence of spectrally active wavelengths necessary to induce this biosynthetic response.

Unlike Souza et al. (2011) [22], who observed no significant effect of colored shade nets on coumarin content in *M. glomerata* leaves, the present study found higher coumarin levels in *M. laevigata* cultivated under red and black nets (Figure 4G). These findings align with Almeida et al. (2017) [76], who reported increased coumarin accumulation in *M. laevigata* under 50% shading, whereas *M. glomerata* exhibited low sensitivity to changes in irradiance. Similarly, Bertolucci et al. (2013) [77] also reported greater coumarin content in *M. laevigata* grown under 80% shading, thereby strengthening the hypothesis that this species responds positively to reduced light availability.

According to Almeida et al. (2017) [76], this phenomenon may be linked to the ecological adaptation of *M. laevigata*, a species native to the Atlantic Forest. This biome is characterized by elevated humidity, frequent rainfall, and attenuated irradiance, primarily due to its dense canopy vegetation [78]. Within this ecological context, the red and black shade nets may have attenuated excess light, replicating environmental conditions similar to the species' natural habitat and consequently alleviating potential photodegradation stress. Coumarin is synthesized through the phenylpropanoid pathway, initiated by the conversion of phenylalanine to trans-cinnamic acid, a reaction catalyzed by phenylalanine ammonia-lyase PAL, whose activity is well-established as being responsive to environmental cues [13,14]. Thus, it is plausible that the diminished solar radiation under these nets promoted the induction of this biosynthetic pathway, leading to greater coumarin accumulation in the leaves.

This outcome aligns with the patterns observed for anthocyanins and the coumarin-to-total chlorophyll ratio (Figure 4H), which were highest under full sunlight, intermediate at the black and red nets, and lowest under the blue net. As this trend mirrored the irradiance levels, it suggests that moderate light favored coumarin synthesis, while both excessive and insufficient light may have been limiting factors. These results reinforce the idea that intermediate irradiance is optimal for secondary metabolism in *M. laevigata* and highlight the relevance of a species' ecological origin in guiding cultivation strategies.

5. Conclusions

This study demonstrates that the use of colored shade nets, particularly red and black, in conjunction with foliar D-limonene application at intermediate concentrations (up to 1.20 mL L^{-1}), constitutes a promising strategy for enhancing plant growth and augmenting the accumulation of bioactive compounds in *Mikania laevigata*. This approach holds significant potential for application in organic agriculture or for integration with other agronomic cultivation practices, thereby improving production system sustainability. Our findings revealed positive morphophysiological responses and a characteristic hormetic effect of D-limonene, underscoring its potential as a biostimulant in medicinal plants. Interestingly, pigment synthesis and the production of pharmacological compounds were predominantly influenced by the light environment rather than by D-limonene application, which highlights the critical role of light quality in modulating key metabolic pathways.

 doi:10.20944/preprints202506.1461.v1

Therefore, future research should prioritize the investigation of the physiological, hormonal, and genetic mechanisms involved in the action of D-limonene, as well as its application across different phenological stages and under field conditions, in order to broaden the understanding of its functionality and practical application.

Author Contributions: Conceptualization, P.H.V.R., M.E.A.S. and V.O.D.; methodology, P.H.V.R. and M.E.A.S.; formal analysis, M.E.A.S. and V.O.D.; resources, P.H.V.R., M.E.A.S. and V.O.D.; data curation, M.E.A.S., V.O.D., J.C.A-J. and G.B.A.; writing—original draft preparation, M.E.A.S., V.O.D., J.C.A-J. and G.B.A.; writing—review and editing P.H.V.R., A.A.B., L.G.Z. and J.A.L.; supervision, P.H.V.R.; project administration, P.H.V.R. All authors have read and agreed to the published version of the manuscript.

Funding: This research was supported by the Brazilian National Council for Scientific and Technological Development (CNPq – processes 2024/1610 and 141286/2023-7), the the São Paulo Research Foundation (FAPESP – process 2012/16932-7), and the Luiz de Queiroz Agricultural Studies Foundation (Fealq).

Data Availability Statement: The data that supports the findings of this study is available from the corresponding authors on reasonable request.

Acknowledgments: The authors thank the Graduate Program in Crop Science at ESALQ/USP for institutional support, and the assistance of Apis Flora®® Industrial and Commercial Ltd.a. in conducting the bioactive compounds analysis.

Conflicts of Interest: L.G.Z., J.A.L and A.A.B. were employed by Apis Flora®® Industrial and Commercial Ltd.a. The remaining authors declare that the research was conducted in the absence of any commercial or financial relationships that could be construed as a potential conflict of interest.

References

1. Singh, P.A.; Bajwa, N.; Chinnam, S.; Chandan, A.; Baldi, A. An overview of some important deliberations to promote medicinal plants cultivation. *J. Appl. Res. Med. Aromat. Plants* **2022**, *31*, https://doi.org/10.1016/j.jarmap.2022.100400.
2. Davis, C.C.; Choisy, P. Medicinal plants meet modern biodiversity science. *Curr. Biol.* **2024**, *34*, R158–R173, https://doi.org/10.1016/j.cub.2023.12.038.
3. Chen, S.-L.; Yu, H.; Luo, H.-M.; Wu, Q.; Li, C.-F.; Steinmetz, A. Conservation and sustainable use of medicinal plants: problems, progress, and prospects. *Chin. Med.* **2016**, *11*, 1–10, https://doi.org/10.1186/s13020-016-0108-7.
4. Wang, W.; Xu, J.; Fang, H.; Li, Z.; Li, M. Advances and challenges in medicinal plant breeding. *Plant Sci.* **2020**, *298*, 110573, https://doi.org/10.1016/j.plantsci.2020.110573.
5. Flor IC; Rodrigues AR; Silva SA; Proença B; Maia VC. Insect Galls on Asteraceae in Brazil: Richness, Geographic Distribution, Associated Fauna, Endemism and Economic Importance. Biota Neotrop 2022, 22, e20211234. https://doi.org/10.1590/1676-0611-bn-2021-1234
6. da Silva RA. Pharmacopéia dos Estados Unidos do Brasil 1st ed Companhia Editora Nacional São Paulo Brazil 1929 p 997
7. Azevedo SGD; Oliveira LPH; Manzali SI; Car SA. Fitoterapia Contemporânea—Tradição e Ciência na Prática Clínica 2nd ed Guanabara Koogan Rio de Janeiro Brazil 2018 pp 286–289
8. Garcia, T.P.; Gorski, D.; Cobre, A.d.F.; Lazo, R.E.L.; Bertol, G.; Ferreira, L.M.; Pontarolo, R. Biological Activities of *Mikania glomerata* and *Mikania laevigata*: A Scoping Review and Evidence Gap Mapping. *Pharmaceuticals* **2025**, *18*, 552, https://doi.org/10.3390/ph18040552.
9. Ortiz, A.; Sansinenea, E. Phenylpropanoid Derivatives and Their Role in Plants' Health and as antimicrobials. *Curr. Microbiol.* **2023**, *80*, 1–13, https://doi.org/10.1007/s00284-023-03502-x.
10. de Souza, J.O.; Oliveira, E.F.; dos Santos, M.E.S.; Kirsten, C.N. Mikania glomerata Spreng. (Asteraceae): seu uso terapêutico e seu potencial na Pandemia de COVID-19. *Rev. Fitos* **2022**, *16*, 270–276, https://doi.org/10.32712/2446-4775.2022.1292.
11. Yatsuda, R.; Rosalen, P.; Cury, J.; Murata, R.; Rehder, V.; Melo, L.; Koo, H. Effects of Mikania genus plants on growth and cell adherence of mutans streptococci. *J. Ethnopharmacol.* **2005**, *97*, 183–189, https://doi.org/10.1016/j.jep.2004.09.042.

 doi:10.20944/preprints202506.1461.v1

12. Rosini, B.; Bulla, A.M.; Polonio, J.C.; Polli, A.D.; da Silva, A.A.; Schoffen, R.P.; de Oliveira-Junior, V.A.; Santos, S.d.S.; Golias, H.C.; Azevedo, J.L.; et al. Isolation, identification, and bioprospection of endophytic bacteria from medicinal plant Mikania glomerata (Spreng.) and the consortium of Pseudomonas as plant growth promoters. *Biocatal. Agric. Biotechnol.* **2025**, https://doi.org/10.1016/j.bcab.2025.103530.
13. Czelusniak, K.; Brocco, A.; Pereira, D.; Freitas, G. Farmacobotânica, fitoquímica e farmacologia do Guaco: revisão considerando Mikania glomerata Sprengel e Mikania laevigata Schulyz Bip. ex Baker. *Rev. Bras. de Plantas Med.* **2012**, *14*, 400–409, https://doi.org/10.1590/s1516-05722012000200022.
14. Alves, L.; Deschamps, C. Radiation levels of UV-A and UV-B on growth parameters and coumarin content in guaco. *Cienc. Rural.* **2019**, *49*, https://doi.org/10.1590/0103-8478cr20190042.
15. Punja, Z.K.; Sutton, D.B.; Kim, T. Glandular Trichome Development, Morphology, and Maturation Are Influenced by Plant Age and Genotype in High THC-Containing Cannabis sativa L. Inflorescences. J. Cannabis Res. 2023, 5, 12. https://doi.org/10.1186/s42238-023-00190-w
16. Thawonkit, T.; Insalud, N.; Dangtungee, R.; Bhuyar, P. Integrating Sustainable Cultivation Practices and Advanced Extraction Methods for Improved Cannabis Yield and Cannabinoid Production. *Int. J. Plant Biol.* **2025**, *16*, 38, https://doi.org/10.3390/ijpb16020038.
17. Souza, G.S.; Castro, E.M.; Soares, A.M.; Pinto, J.E.B.P. Biometric and physiological aspects of young plants of Mikania glomerata Sprengel and Mikania laevigata Schultz Bip. ex Baker under colored nets. Rev. Bras. Biociênc. 2010, 8, 330–335.
18. Thakur, M.; Kumar, R. Microclimatic buffering on medicinal and aromatic plants: A review. *Ind. Crop. Prod.* **2021**, *160*, https://doi.org/10.1016/j.indcrop.2020.113144.
19. Contin, D.R.; Habermann, E.; Alves, V.M.; Martinez, C.A. Morpho-physiological performance of Mikania glomerata Spreng. and Mikania laevigata Sch. Bip ex Baker plants under different light conditions. *Hoehnea* **2021**, *48*, https://doi.org/10.1590/2236-8906-74/2020.
20. Ahemd, H.A.; Al-Faraj, A.A.; Abdel-Ghany, A.M. Shading greenhouses to improve the microclimate, energy and water saving in hot regions: A review. *Sci. Hortic.* **2016**, *201*, 36–45, https://doi.org/10.1016/j.scienta.2016.01.030.
21. Freire, M.M.; Rodrigues, P.H.V.; Duarte, S.N.; Barros, T.H.d.S.; Brito, G.B.d.S.; Marques, P.A.A. Influence of Colored Shade Nets and Salinity on the Development of Roselle Plants. *Agronomy* **2024**, *14*, 2252, https://doi.org/10.3390/agronomy14102252.
22. Souza, G.S.; Pinto, J.E.B.P.; Resende, M.G.; Bertolucci, S.K.V.; Soares, Â.M.; Castro, E.M. Crescimento, teor de óleo essencial e conteúdo de cumarina de plantas jovens de gauco (Mikania glomerata Sprengel) cultivadas sob malhas coloridasDOI: 10.5007/2175-7925.2011v24n3p1. *Biotemas* **2011**, *24*, 1–11, https://doi.org/10.5007/2175-7925.2011v24n3p1.
23. Thakur, M.; Bhattacharya, S.; Khosla, P.K.; Puri, S. Improving production of plant secondary metabolites through biotic and abiotic elicitation. *J. Appl. Res. Med. Aromat. Plants* **2019**, *12*, 1–12, https://doi.org/10.1016/j.jarmap.2018.11.004.
24. Chaimovitsh, D.; Shachter, A.; Abu-Abied, M.; Rubin, B.; Sadot, E.; Dudai, N. Herbicidal Activity of Monoterpenes Is Associated with Disruption of Microtubule Functionality and Membrane Integrity. *Weed Sci.* **2016**, *65*, 19–30, https://doi.org/10.1614/ws-d-16-00044.1.
25. De Souza T, Ferreira JV, Damaso DC, Vasconcelos PS, Lima AM, Perfeito JPS. Uso de cascas de laranja para extração de óleo essencial e avaliação de suas atividades biológicas. Rev Ifes Ciênc. 2024;10(1):1–23. https://orcid.org/0000-0002-6667-1806
26. Orsi, B.; Demétrio, C.A.; Jacob, J.F.O.; Rodrigues, P.H.V. Effect of terpene treatment on tomato fruit. *Bragantia* **2022**, *81*, https://doi.org/10.1590/1678-4499.20210134.
27. Alvares, C.A.; Stape, J.L.; Sentelhas, P.C.; Moraes, G.J.L.; Sparovek, G. Köppen's climate classification map for Brazil. *Meteorol. Z.* **2013**, *22*, 711–728, doi:10.1127/0941-2948/2013/0507.
28. Hiscox, J.D.; Israelstam, G.F. A method for the extraction of chlorophyll from leaf tissue without maceration. *Can. J. Bot.* **1979**, *57*, 1332–1334, https://doi.org/10.1139/b79-163.
29. Lees, D.H.; Francis, F.J. Effect of Gamma Radiation on Anthocyanin and Flavonol Pigments in Cranberries (Vaccinium macrocarpon Ait.)1. *J. Am. Soc. Hortic. Sci.* **1972**, *97*, 128–132, https://doi.org/10.21273/jashs.97.1.128.

 doi:10.20944/preprints202506.1461.v1

30. Siegelman, H.W.; Hendricks, S.B. Photocontrol of Anthocyanin Synthesis in Apple Skin.. *Plant Physiol.* **1958**, *33*, 185–190, https://doi.org/10.1104/pp.33.3.185.
31. de Medeiros, J.; Kanis, L.A. Avaliação do efeito de polietilenoglicóis no perfil de extratos de Mikania glomerata Spreng., Asteraceae, e Passiflora edulis Sims, Passifloraceae. *Rev. Bras. de Farm.* **2010**, *20*, 796–802, https://doi.org/10.1590/s0102-695x2010005000001.
32. Francisco, d.A.S.e.S.; Carlos, A.V.d.A. The Assistat Software Version 7.7 and its use in the analysis of experimental data. *Afr. J. Agric. Res.* **2016**, *11*, 3733–3740, https://doi.org/10.5897/ajar2016.11522.
33. Honorato, A.d.C.; Nohara, G.A.; de Assis, R.M.; Maciel, J.F.; de Carvalho, A.A.; Pinto, J.E.; Bertolucci, S.K. Colored shade nets and different harvest times alter the growth, antioxidant status, and quantitative attributes of glandular trichomes and essential oil of Thymus vulgaris L.. *J. Appl. Res. Med. Aromat. Plants* **2023**, *35*, https://doi.org/10.1016/j.jarmap.2023.100474.
34. de Oliveira, J.E.; Sabino, J.H.F.; Sillmann, T.A.; Mattiuz, C.F.M. Cultivation under photoselective shade nets alters the morphology and physiology of Begonia Megawatt varieties. *Cienc. E Agrotecnologia* **2024**, *48*, e015924, https://doi.org/10.1590/1413-7054202448015924.
35. Dickson, R.; Fisher, P. Quantifying the effects of fifteen floriculture species on substrate-pH. *Acta Hortic.* **2019**, 337–344, https://doi.org/10.17660/actahortic.2019.1266.47.
36. Vuković, M.; Jurić, S.; Bandić, L.M.; Levaj, B.; Fu, D.-Q.; Jemrić, T. Sustainable Food Production: Innovative Netting Concepts and Their Mode of Action on Fruit Crops. *Sustainability* **2022**, *14*, 9264, https://doi.org/10.3390/su14159264.
37. Kabir, Y.; Nambeesan, S.U.; Díaz-Pérez, J.C. Shade nets improve vegetable performance. *Sci. Hortic.* **2024**, *334*, https://doi.org/10.1016/j.scienta.2024.113326.
38. Tittonell, P.; Giller, K.E. When yield gaps are poverty traps: The paradigm of ecological intensification in African smallholder agriculture. *Field Crop. Res.* **2013**, *143*, 76–90, https://doi.org/10.1016/j.fcr.2012.10.007.
39. Sharma, A.; Shahzad, B.; Rehman, A.; Bhardwaj, R.; Landi, M.; Zheng, B. Response of Phenylpropanoid Pathway and the Role of Polyphenols in Plants under Abiotic Stress. *Molecules* **2019**, *24*, 2452, doi:10.3390/molecules24132452.
40. Li, Z.; Ahammed, G.J. Plant stress response and adaptation via anthocyanins: A review. *Plant Stress* **2023**, *10*, https://doi.org/10.1016/j.stress.2023.100230.
41. Song, S.; He, A.; Zhao, T.; Yin, Q.; Mu, Y.; Wang, Y.; Liu, H.; Nie, L.; Peng, S. Effects of shading at different growth stages with various shading intensities on the grain yield and anthocyanin content of colored rice (Oryza sativa L.). *Field Crop. Res.* **2022**, *283*, https://doi.org/10.1016/j.fcr.2022.108555.
42. Han, S.; Liu, Y.; Bao, A.; Jiao, T.; Zeng, H.; Yue, W.; Yin, L.; Xu, M.; Lu, J.; Wu, M.; et al. A Characterization of the Functions of OsCSN1 in the Control of Sheath Elongation and Height in Rice Plants under Red Light. *Agronomy* **2024**, *14*, 572, https://doi.org/10.3390/agronomy14030572.
43. Dubois, P.G.; Brutnell, T.P. Topology of a maize field. *Plant Signal. Behav.* **2011**, *6*, 467–470, https://doi.org/10.4161/psb.6.4.14305.
44. Harish, B.; Umesha, K.; Venugopalan, R.; Prasad, B.M. Photo-selective nets influence physiology, growth, yield and quality of turmeric (Curcuma longa L.). *Ind. Crop. Prod.* **2022**, *186*, https://doi.org/10.1016/j.indcrop.2022.115202.
45. Zhang, Q.; Bi, G.; Li, T.; Wang, Q.; Xing, Z.; LeCompte, J.; Harkess, R.L. Color Shade Nets Affect Plant Growth and Seasonal Leaf Quality of Camellia sinensis Grown in Mississippi, the United States. *Front. Nutr.* **2022**, *9*, 786421, https://doi.org/10.3389/fnut.2022.786421.
46. dos Santos, L.D.G.; da Rosa, G.G.; Lima, C.S.M.; Bonome, L.T.d.S. Colorações de malhas de sombreamento sobre a fenologia, biometria e características físico-químicas de Physalis peruviana L. em sistema orgânico de produção. **2023**, *22*, 285–294, https://doi.org/10.5965/223811712222023285.
47. Costa, L.C.D.B.; Pinto, J.E.B.P.; de Castro, E.M.; Alves, E.; Bertolucci, S.K.V.; Rosal, L.F. Effects of coloured shade netting on the vegetative development and leaf structure of Ocimum selloi. *Bragantia* **2010**, *69*, 349–359, https://doi.org/10.1590/s0006-87052010000200012.
48. Ilić, Z.S.; Milenković, L.; Šunić, L.; Barać, S.; Mastilović, J.; Kevrešan, Ž.; Fallik, E. Effect of shading by coloured nets on yield and fruit quality of sweet pepper. *Zemdirbyste-Agriculture* **2016**, *104*, 53–62, https://doi.org/10.13080/z-a.2017.104.008.

 doi:10.20944/preprints202506.1461.v1

49. Costa, A.G.; Chagas, J.H.; Pinto, J.E.B.P.; Bertolucci, S.K.V. Crescimento vegetativo e produção de óleo essencial de hortelã-pimenta cultivada sob malhas. *Pesqui. Agropecu. Bras.* **2012**, *47*, 534–540, https://doi.org/10.1590/s0100-204x2012000400009.
50. Luz, J.M.Q.; dos Santos, A.P.; de Oliveira, R.C.; Blank, A.F. Optimizing in vitro growth of basil using LED lights. *Cienc. Rural.* **2023**, *53*, https://doi.org/10.1590/0103-8478cr20220030.
51. Taiz, L.; Zeiger, E.; Møller, I.M.; Murphy, A. Plant Physiology and Development, 6th ed.; Sinauer As-sociates, Inc.: Sunderland, MA, USA, 2015.
52. Zhou, T.; Chang, F.; Li, X.; Yang, W.; Huang, X.; Yan, J.; Wu, Q.; Wen, F.; Pei, J.; Ma, Y.; et al. Role of auxin and gibberellin under low light in enhancing saffron corm starch degradation during sprouting. *Int. J. Biol. Macromol.* **2024**, *279*, 135234, https://doi.org/10.1016/j.ijbiomac.2024.135234.
53. Kurepin, L.V.; Emery, R.J.N.; Pharis, R.P.; Reid, D.M. The interaction of light quality and irradiance with gibberellins, cytokinins and auxin in regulating growth of *Helianthus annuus* hypocotyls. *Plant, Cell Environ.* **2006**, *30*, 147–155, https://doi.org/10.1111/j.1365-3040.2006.01612.x.
54. Ribeiro, F.N.S.; de Assis, R.M.A.; Leite, J.J.F.; Miranda, T.F.; Alves, E.; Bertolucci, S.K.V.; Pinto, J.E.B.P. The cultivation of Lippia dulcis under ChromatiNet induces changes in vegetative growth, anatomy and essential oil chemical composition. *South Afr. J. Bot.* **2024**, *174*, 393–404, https://doi.org/10.1016/j.sajb.2024.09.003.
55. Ribeiro, A.S.; Ribeiro, M.S.; Bertolucci, S.K.; Bittencourt, W.J.; DE Carvalho, A.A.; Tostes, W.N.; Alves, E.; Pinto, J.E. Colored shade nets induced changes in growth, anatomy and essential oil of Pogostemon cablin. *An. da Acad. Bras. de Cienc.* **2018**, *90*, 1823–1835, https://doi.org/10.1590/0001-3765201820170299.
56. Vargas-Hernandez, M.; Macias-Bobadilla, I.; Guevara-Gonzalez, R.G.; Romero-Gomez, S.d.J.; Rico-Garcia, E.; Ocampo-Velazquez, R.V.; Alvarez-Arquieta, L.d.L.; Torres-Pacheco, I. Plant Hormesis Management with Biostimulants of Biotic Origin in Agriculture. *Front. Plant Sci.* **2017**, *8*, 1762, https://doi.org/10.3389/fpls.2017.01762.
57. Pannacci, E.; Baratta, S.; Falcinelli, B.; Farneselli, M.; Tei, F. Mugwort (*Artemisia vulgaris* L.) Aqueous Extract: Hormesis and Biostimulant Activity for Seed Germination and Seedling Growth in Vegetable Crops. *Agriculture* **2022**, *12*, 1329, https://doi.org/10.3390/agriculture12091329.
58. Pannacci, E.; Onofri, A.; Covarelli, G. Biological activity, availability and duration of phytotoxicity for imazamox in four different soils of central Italy. *Weed Res.* **2006**, *46*, 243–250, https://doi.org/10.1111/j.1365-3180.2006.00503.x.
59. Belz, R.G.; O Duke, S. Herbicides and plant hormesis. *Pest Manag. Sci.* **2014**, *70*, 698–707, https://doi.org/10.1002/ps.3726.
60. Lin, H.; Li, Z.; Sun, Y.; Zhang, Y.; Wang, S.; Zhang, Q.; Cai, T.; Xiang, W.; Zeng, C.; Tang, J. D-Limonene: Promising and Sustainable Natural Bioactive Compound. *Appl. Sci.* **2024**, *14*, 4605, https://doi.org/10.3390/app14114605.
61. Ninkuu, V.; Zhang, L.; Yan, J.; Fu, Z.; Yang, T.; Zeng, H. Biochemistry of Terpenes and Recent Advances in Plant Protection. *Int. J. Mol. Sci.* **2021**, *22*, 5710, https://doi.org/10.3390/ijms22115710.
62. Hasan, S.A.; Irfan, M.; Masrahi, Y.; Khalaf, M.A.; Hayat, S.; Moral, M.T. Growth, photosynthesis, and antioxidant responses of Vigna unguiculata L. treated with hydrogen peroxide. *Cogent Food Agric.* **2016**, *2*, https://doi.org/10.1080/23311932.2016.1155331.
63. Sbaghi, M.; el Aalaoui, M. Evaluating natural product-based herbicides for effective control of invasive water lettuce (Pistia stratiotes L.). Adv. Weed Sci. 2025, 43, 00001. https://doi.org/10.51694/AdvWeedSci/2025;43:00001
64. Gettys, L.A.; Thayer, K.L.; Sigmon, J.W. Evaluating the Effects of Acetic Acid and d-Limonene on Four Aquatic Plants. *HortTechnology* **2021**, *31*, 225–233, https://doi.org/10.21273/horttech04769-20.
65. Sieniawska, E.; Swatko-Ossor, M.; Sawicki, R.; Ginalska, G. Morphological Changes in the Overall Mycobacterium tuberculosis H37Ra Cell Shape and Cytoplasm Homogeneity due to Mutellina purpurea L. Essential Oil and Its Main Constituents. *Med Princ. Pr.* **2015**, *24*, 527–532, https://doi.org/10.1159/000439351.
66. Han, Y.; Sun, Z.; Chen, W. Antimicrobial Susceptibility and Antibacterial Mechanism of Limonene against *Listeria monocytogenes*. *Molecules* **2019**, *25*, 33, https://doi.org/10.3390/molecules25010033.
67. Díaz-Pérez, J.C.; John, K.S. Bell Pepper (Capsicum annum L.) under Colored Shade Nets: Plant Growth and Physiological Responses. *HortScience* **2019**, *54*, 1795–1801, https://doi.org/10.21273/hortsci14233-19.

 doi:10.20944/preprints202506.1461.v1

68. Zoratti, L.; Jaakola, L.; Häggman, H.; Giongo, L.; Xu, C. Modification of Sunlight Radiation through Colored Photo-Selective Nets Affects Anthocyanin Profile in Vaccinium spp. Berries. *PLOS ONE* **2015**, *10*, e0135935, https://doi.org/10.1371/journal.pone.0135935.
69. Wolske, E.; Chatham, L.; Juvik, J.; Branham, B. Berry Quality and Anthocyanin Content of 'Consort' Black Currants Grown under Artificial Shade. *Plants* **2021**, *10*, 766, https://doi.org/10.3390/plants10040766.
70. Feitosa, L.G.P.; Monge, M.; Lopes, N.P.; de Oliveira, D.C.R. Distribution of flavonoids and other phenolics in Mikania species (Compositae) of Brazil. *Biochem. Syst. Ecol.* **2021**, *97*, https://doi.org/10.1016/j.bse.2021.104273.
71. Ye, J.-H.; Lv, Y.-Q.; Liu, S.-R.; Jin, J.; Wang, Y.-F.; Wei, C.-L.; Zhao, S.-Q. Effects of Light Intensity and Spectral Composition on the Transcriptome Profiles of Leaves in Shade Grown Tea Plants (*Camellia sinensis* L.) and Regulatory Network of Flavonoid Biosynthesis. *Molecules* **2021**, *26*, 5836, https://doi.org/10.3390/molecules26195836.
72. Wang, Y.; Gao, L.; Shan, Y.; Liu, Y.; Tian, Y.; Xia, T. Influence of shade on flavonoid biosynthesis in tea (Camellia sinensis (L.) O. Kuntze). *Sci. Hortic.* **2012**, *141*, 7–16, https://doi.org/10.1016/j.scienta.2012.04.013.
73. Jiménez-Viveros, Y.; Núñez-Palenius, H.G.; Fierros-Romero, G.; Valiente-Banuet, J.I. Modification of Light Characteristics Affect the Phytochemical Profile of Peppers. *Horticulturae* **2023**, *9*, 72, https://doi.org/10.3390/horticulturae9010072.
74. Hashemi, S.M.B.; Kamani, M.H.; Amani, H.; Khaneghah, A.M. Voltage and NaCl concentration on extraction of essential oil from Vitex pseudonegundo using ohmic-hydrodistillation. *Ind. Crop. Prod.* **2019**, *141*, https://doi.org/10.1016/j.indcrop.2019.111734.
75. Fu, B.; Ji, X.; Zhao, M.; He, F.; Wang, X.; Wang, Y.; Liu, P.; Niu, L. The influence of light quality on the accumulation of flavonoids in tobacco (Nicotiana tabacum L.) leaves. *J. Photochem. Photobiol. B: Biol.* **2016**, *162*, 544–549, https://doi.org/10.1016/j.jphotobiol.2016.07.016.
76. Almeida, C.d.L.; Xavier, R.M.; Borghi, A.A.; dos Santos, V.F.; Sawaya, A.C.H.F. Effect of seasonality and growth conditions on the content of coumarin, chlorogenic acid and dicaffeoylquinic acids in Mikania laevigata Schultz and Mikania glomerata Sprengel (Asteraceae) by UHPLC–MS/MS. *International Journal of Mass Spectrometry* **2017**, *418*, 162–172, https://doi.org/10.1016/j.ijms.2016.09.016.
77. Bertolucci, S.K.V.; Pereira, A.B.D.; Pinto, J.E.B.P.; Oliveira, A.B.; Braga, F.C. Seasonal Variation on the Contents of Coumarin and Kaurane-Type Diterpenes in *Mikania laevigata* and *M. glomerata* Leaves under Different Shade Levels. *Chem. Biodivers.* **2013**, *10*, 288–295, https://doi.org/10.1002/cbdv.201200166.
78. Gasparetto, J.C.; Campos, F.R.; Budel, J.M.; Pontarolo, R. Mikania glomerata Spreng. e M. laevigata Sch. Bip. ex Baker, Asteraceae: estudos agronômicos, genéticos, morfoanatômicos, químicos, farmacológicos, toxicológicos e uso nos programas de fitoterapia do Brasil. *Rev. Bras. de Farm.* **2010**, *20*, 627–640, https://doi.org/10.1590/s0102-695x2010000400025.